Proceedings of the
American Control Conference
Seattle, Washington • June 1995

Multiobjective Optimization of Hard Disk Suspension Assemblies: Part II - Integrated Structure and Control Design

Yee-Pien Yang and Yi-An Chen
Department of Mechanical Engineering
National Taiwan University
Taipei, Taiwan 10764, R.O.C.
02-363-0231 Ext.2175 ypyang@w3.me.ntu.edu.tw

Abstract

The design of actively controlled hard disk suspension assemblies is formulated as a multiobjective optimization problem. The integrated structure/control objectives consist of natural frequencies and an optimal control performance index with weighted system state regulation errors and control efforts, subject to some side constraints on design variables that describe the geometry of the suspension. Two multiobjective optimization techniques, goal programming and compromise programming, are implemented through an interface program communicating with an advanced finite element analysis program. The feasibility of the optimal design is demonstrated and the final decision making is also discussed.

1. Introduction

The flying height of the slider over the rotating disk always dominates the record density, hence the size, weight and capacity of a hard disk drive. The fluctuation of the flying height is inevitable during the disk operation, stemming from disturbances such as vibrations of actuator arm, rotating flow induced vibrations, lateral positioning motion induced out-of-plane vibrations, inaccuracies of spindle alignment, and so on. Either passive design or active control on the suspension assembly can be used to reduce the suspension vibration, thereby keeping the flying height as small as possible. However, better structural designs usually facilitate the implementation of active vibration controls, which would have less effort than controlling a structure without optimal designs. Moreover, the inclusion of the control performance in the structural optimization must result in more feasible designs. This motivates many researchers devoting themselves to the integrated structure and control optimization technique, and this has received tremendous attention in recent years, due to the increasing demands on the reduction of structure weight and control effort, and on the improvement of closed-loop system response. Several approaches are being developed and used in the design and control optimization problems, and these can be broadly classified as 1) sequential optimization, 2) simultaneous optimization, and 3) multiobjective optimization and other optimization techniques.

The sequential optimization technique carries out first the structural (or control) design followed sequentially by the control (or structural) design. The drawback of this approach is that the integrated solution depends on the sequential ordering of the control and structure design solutions. The simultaneous optimization technique allows the designer to formulate a performance index, in structural parameters and control variables, as the sum of structural properties, such as mass or fundamental frequency, and the quadratic performance index associated with a linear regulator optimal control problem. Usually there exists no unique solution that would give the optimum for all objective functions simultaneously.

Various multiobjective optimization techniques have been proposed and applied in the industry, as surveyed by Tseng and Lu (1994). For the application to the combined structure/control optimization, Rao et al. (1988) used the cooperative game theory for the design of actively controlled structures subject to the constraints on damping parameters of the closed-loop system, formulating a multiobjective optimization problem. The structural weight and control energy were objective functionals for minimization with cross-sectional areas of members as design variables. Livne et al. (1990) formulated the synthesis of actively controlled composite wing as a multidisciplinary optimization problem, where a unique integration of analysis techniques spanning the diciplines of structures, aerodynamics, and controls is described. Gilbert and Schmidt (1991) proposed a multilevel optimization approach to the integrated structure/control law design. The lower level consisted of independent structural design and control law design, and the design results and sensitivities were coordinated through the upper level optimization problem that reflected the desired objectives of the integrated structure/control law design.

The goal of Part II is to integrate structure and control optimization techniques on the shape design of suspension assemblies of hard disks. The design objective is to raise natural frequencies of the suspension assembly so that it will not be excited easily by undesirable disturbances, as stated in Part I. Simultaneously, the state regulation errors and vibration

control efforts are minimized with respect to structural parameters as well as control gains. Since Part I has to be refereed, the numbers of equations and appendices will continue.

2. Optimal Control of Parametric Equations

2.1. Modal Analysis

In this section a generic class of optimization problems is defined specifically for vibration control of flexible structures. In terms of design variables $\mathbf{x}$, the Nth-order equations of motion (1) that describe the dynamic behavior of the suspension assembly can be transformed to principal (modal) coordinates

$$\ddot{\eta} + C'(\mathbf{x})\dot{\eta} + K'(\mathbf{x})\eta = B'(\mathbf{x})\mathbf{u} \tag{7}$$

by the matrix transformation

$$\mathbf{q} = \Phi(\mathbf{x})\eta \tag{8}$$

where η is the modal coordinate vector, $\Phi(\mathbf{x})$ is the modal matrix whose columns are the corresponding normal modes, that is,

$$\Phi(\mathbf{x}) = [\phi_1, \phi_2, ...\phi_N]. \tag{9}$$

For simplicity, the argument $\mathbf{x}$ is omitted for subsequent analyses. The matrices K', C' an B' have been normalized, that we call the modal stiffness, modal damping, and modal input influence matrices, respectively, given by

$$K' = [\mathbf{m}]^{-1}\Phi^T K\Phi = diag(\omega_1^2 \;\; \omega_2^2 \;\; ... \;\; \omega_N^2) \tag{10}$$

$$C' = [\mathbf{m}]^{-1}\Phi^T C\Phi = diag(2\zeta_1\omega_1 \;\; 2\zeta_2\omega_2 \;\; ... \;\; 2\zeta_N\omega_N) \tag{11}$$

$$B' = [\mathbf{m}]^{-1}\Phi^T B \tag{12}$$

in which

$$[\mathbf{m}] = \Phi^T M\Phi = diag(m_1 \;\; m_2 \;\; ... \;\; m_N) \tag{13}$$

is a diagonal modal mass matrix, ζ_i and ω_i are the damping ratio and natural frequency of the ith normal mode.

2.2. Optimal Control Formulation

By the modal analysis the transformation to principal coordinates has uncoupled the equations of motion, leading to N separate single-degrees-of-freedom equations. In fact, high-frequency modes possess less kinetic and potential energy, and decay much faster than low-frequency modes due to the structural damping. It is efficient and practical for the designer to truncate those modal coordinates that correspond to high-frequency modes. In the following optimal control formulation, selected are S modal coordinates that describe the dominant dynamic behavior of the suspension assembly. In the state-space form, Eq.(7) is expressed by

$$\dot{\mathbf{y}} = \mathbf{A}\mathbf{y} + \mathbf{B}\mathbf{u} \tag{14}$$

where $\mathbf{y} = [\eta^T \;\; \dot{\eta}^T]^T$ is the state variable vector, and $\mathbf{A}$ and $\mathbf{B}$ are the plant and input matrices given by

$$\mathbf{A} = \begin{bmatrix} 0 & I \\ -K' & -C' \end{bmatrix} \text{ and } \mathbf{B} = \begin{bmatrix} 0 \\ B' \end{bmatrix}. \tag{15}$$

In order to design a linear quadratic regulator a performance index (PI) can be defined as

$$f_4 = \frac{1}{2}\int_0^\infty (\bar{\mathbf{q}}^T\mathbf{Q}\bar{\mathbf{q}} + \mathbf{u}^T\mathbf{R}\mathbf{u})dt \tag{16}$$

where $\bar{\mathbf{q}} = [\mathbf{q}^T \;\; \dot{\mathbf{q}}^T]^T$, and $\mathbf{Q}$ and $\mathbf{R}$ are the state and control weighting matrices which have to be positive semi-definite and positive definite, respectively. Suppose that the system is either uniformly completely controllable or exponentially stable, the minimization of the performance index for a set of design variables yields the steady-state optimal control law

$$\mathbf{u}^* = -\mathbf{R}^{-1}\mathbf{B}^T\mathbf{P}\mathbf{y} \tag{17}$$

where $\mathbf{P}$ is the Riccati matrix that satisfies the algebraic equation

$$\mathbf{A}^T\mathbf{P} + \mathbf{P}\mathbf{A} - \mathbf{P}\mathbf{B}\mathbf{R}^{-1}\mathbf{B}^T\mathbf{P} + \Phi_d^T\mathbf{Q}\Phi_d = 0 \tag{18}$$

in which $\Phi_d = diag(\Phi \; \Phi)$. Therefore, the governing equation of the optimum closed-loop system can be written as

$$\dot{\mathbf{y}} = \bar{\mathbf{A}}\mathbf{y} \tag{19}$$

where

$$\bar{\mathbf{A}} = \mathbf{A} - \mathbf{B}\mathbf{R}^{-1}\mathbf{B}^T\mathbf{P}. \tag{20}$$

2.3. Dynamical Responses

The above optimal control formulation can be used in two ways. First, the optimal control analysis is performed after the structure optimization is completed; that is, the optimal shape of the suspension assembly is determined by minimizing the objective functions f_1, f_2 and f_3 defined in Eq. (2), and then the control responses are examined. On the other words, the optimization will be carried out independently with dual sets of objective functions. Second, all the objective functions $f_i, i = 1$ to 4 are considered simultaneously in the multiobjective optimization techniques: goal programming and compromise programming.

Since the major vibrations of the suspension assembly are exerted by the disturbances from either the air-bearing fluctuations or the rotating flow between disks. The disturbance force distribution depends on the preload of the suspension, flying height, track location of the slider, rotation speed of the disk, and so on. The displacement response is investigated at the slider head with respect to disturbance force inputs at three different locations on the suspension assembly, as shown in Fig. 3. The transfer functions between these disturbance inputs (forces) and the slider head output (displacement) are first computed by selecting the first six modes of the original suspension assembly. It is apparent that the disturbance input point a, near the centroid of the suspension beam, produces the most oscillation on the slider head, while the disturbance input at point c on the slider only slightly excites the head because of the large stiffness of the air bearing.

2.4. Optimal Control Responses

For better control performance with less control effort, two input points are selected for simulation, that we chose the same as disturbance input points a and b. It is true that the symmetric torsional modes are uncontrollable if the inputs act on the nodal lines of the suspension. However, the fundamental mode is usually a bending mode whose magnitude is much larger than that of high-frequency modes, and is a major part of vibrations to suppress.

As the optimal control strategy is performed, the weighting matrices R and Q are chosen so that R=1 and all elements of Q are zeros except $Q_{kk} = 10^{15}$, the diagonal element corresponding to the output displacement point O. By substituting the optimal control u^* of (17) into (7), and calculating the closed-loop transfer functions for output point O with respect to input points a and b, we obtain their frequency responses as shown in Fig. 9. The input points a and b are respectively close to the maximum magnitudes of the first (bending) mode and the second bending (the fourth) mode. It is not surprising that the magnitudes of the first two bending modes (the first and fourth modes) are effectively reduced, in comparison with the frequency response of the uncontrolled system that the dashed curve describes. Moreover, time responses of the optimal control performance compared with the uncontrolled (open-loop) response are presented in Fig. 10, associated with its optimal control effort. Note that for the regulation control of the suspension the initial displacement of the slider head is given as $0.05\mu m$, around $15 \sim 25\%$ of the usual flying height $0.2 \sim 0.3\mu m$.

3. Integrated Optimal Structure and Control Design

3.1. Multifunctional Objectives

As we had in Part I, the shape of the suspension assembly is designed at its loaded status. Both objectives, to keep away from the excitation of disturbances and to actively suppress undesirable vibrations, motivate the designer to choose additional cost function f_4 of Eq.(16) along with the previous cost functions f_1, f_2 and f_3, subject to the side constraints. The computational flow of the optimization, along with the structural analysis and the optimal control, is illustrated in Fig. 11.

3.2. Optimization Results

For comparing with the results obtained in Part I, the same weightings of the two multifunctional optimization techniques are used. Both the indices β and γ are chosen as 1 and 2 for goal and compromise programmings, respectively. The optimization results are shown in Tables 4 and 5, and the optimal shapes in the finite element mesh for the cases of $\beta = 1$ and $\gamma = 1$ are illustrated in Fig. 12.

We conclude in the following comments:

(1) All the flap heights in the optimal design have a maximum allowable value $0.8mm$, except for the case $\beta = 1$ of the goal programming to get a little smaller value $0.7922mm$. It is still hard to tell which case is better, that the designer has to make a final decision with additional dynamical and manufacturing requirements on the suspension assembly.

(2) As in Part I, the final results in raising natural frequencies are satisfactory. Without changing the original length, thickness and tip width of the suspension beam, the first and second natural frequencies are raised over 400 to 500 Hz, and the difference between the second and the third natural frequencies increases at least 500 Hz.

(3) The final value of each objective function, as shown in Table 4 and 5, is larger than its minimum value and less than its maximum value. It is obvious that the nondominated solutions, or superior solutions, are not achieved, but a set of optimal solutions are obtained by making compromise between objective functions with each other.

Table 4: Structure/control optimization design results with goal programming

	β=1	β=2
Design Variable (mm)		
yb	6.8729	6.8509
xd	0.5000	0.5000
$x2$	0.1000	0.2890
wh	0.7922	0.8000
Objectives		
f_1	4.0117e-4	3.9808e-4
f_2	3.9364e-4	3.8969e-4
f_3	2.9614e-4	2.9570e-4
f_4	1.9497e-4	2.0562e-4
Frequencies (Hz)		
ω_1	2493	2512
ω_2	2540	2566
ω_3	5917	5948

Table 5: Structure/control optimization design results with compromise programming

(α=1)	γ=1	γ=2
Design Variable (mm)		
yb	6.0216	5.9600
xd	2.6373	2.8549
$x2$	0.1000	0.2835
wh	0.8000	0.8000
Objectives		
f_1	3.8084e-4	3.9119e-4
f_2	3.4885e-4	3.4209e-4
f_3	3.9303e-4	3.9934e-4
f_4	2.0224e-4	2.0718e-4
Frequencies (Hz)		
ω_1	2626	2556
ω_2	2867	2923
ω_3	5411	5427

4. Decision Making

In the above analyses, we have more than one alternative of optimal designs. The decision maker needs to select the most desirable alternative, and his rational choice requires a criterion by which he evaluates different alternatives and place them in some form of ranking. Back to the original design objectives, the natural frequencies of the suspension assembly have to be raised so that it will not be excited easily by undesirable disturbances. A little different from Part I, we investigate the closed-loop frequency responses of the optimal suspension shape with optimal controls. The single input point is selected at a, and the output is chosen at O where the slider head displacement is measured, as shown in Fig. 3. That way the symmetrical torsional modes are uncontrollable but observable. This will not cause system instability because that the torsional modes are seldom excited by out-of-plane disturbances that produce flying height fluctuations, and that those high-frequency torsional modes will decay fast due to the structural damping.

Figure 13 shows the closed-loop frequency responses of the suspension designed by goal programming ($\beta = 1$) and compromise programming ($\gamma = 1$), respectively, compared to the frequency response of the original suspension with an optimal control. It is interesting to find out that the low-frequency gain of the design with compromise programming is the smallest, while that with goal programming is the largest. This indicates that low-frequency disturbances may bring about less fluctuation of the slider head with the compromise programming design than the other two designs. Moreover, the frequency response with the compromise programming design has more attenuation for higher frequencies, and a little larger bandwidth than that of goal programming design.

It is also necessary to convince people that the control performance of the suspension assembly designed with integrated structure/control optimization is superior to that without optimal control cost in the design as in Part I. Figure 14 is the frequency response of the suspension assembly with goal programming design. The solid curve (design+control) represents the case that the optimal control law is applied to the suspension designed with the objectives f_1, f_2 and f_3, while the dashdot curve (design/control) describes the closed-loop system frequency response with integrated optimization of structure and control. Both frequency responses have almost the same peak value and bandwidth, that is, the same frequency of input at which the output is attenuated to a factor 0.707 times the input. This is verified in Fig. 15 that both time responses have a similar rise time. However, the integrated structure/control design gives much smaller resonant peak in frequency, that introduces more damping and leads to less settling time and less control effort in the regulation control. Similar results appears in the compromise programming design as shown in Figs. 16 and 17.

5. Summary and Conclusions

The integrated structure/control multiobjective optimization of the suspension assembly of hard disk drives has been presented. In addition to the objective functions of nature frequencies as depicted in Part I, also incorporated in the optimization is an optimal control performance index consisting of weighted system state regulation errors and control efforts. Two kinds of objectives have been achieved. First, the first and second natural frequencies are raised and the difference between the second and the third natural frequencies increases, that the suspension is not easily excited by undesirable disturbances. Second, as a vibration controller is implemented it is required that the vibration be suppressed in minimal time and with least control effort. Both the goal programming and compromise programming techniques give feasible solutions, which would not be ideal, but the closest to the ideal ones in the sense that a best compromise is made among objectives. Furthermore, the final decision making requires more investigation on the closed-loop frequency and time responses. For the design of actively controlled structures, the control performances with the integrated structure/control optimization design are superior to those without the optimal control performance index in the design. The final solution may not be unique, but depends on additional engineering experience, manufacturing requirements, and so on.

Acknowledgment

This research was supported by National Science Council under Contract No. NSC 82-0401-E-002-380.

References

Gilbert, M. G. and Schmidt, D. K., 1991, "Integrated Structure/Control Law Design by Multilevel Optimization," *J. Guidance*, Vol. 14, No. 5, pp. 1001-1006.

Livne, E., Schmit, L. A. and Friedmann, P. P., 1990, "Towards Integrated Multidisciplinary Synthesis of Actively Controlled Fiber Composite Wings," Vol. 27, No. 12, December, pp. 979-992.

Rao, S. S., Venkayya, V. B. and Khot, N. S., 1988, "Game Theory Approach for the integrated Design of Structures and Controls," *AIAA Journal*, Vol. 26, No. 4, pp. 463-469.

Tseng, C. H. and Lu, T. W., 1994, "Multiobjective Optimization in Mechanical and Structural Design," to appear in *Modelling and Scientific Computing*.

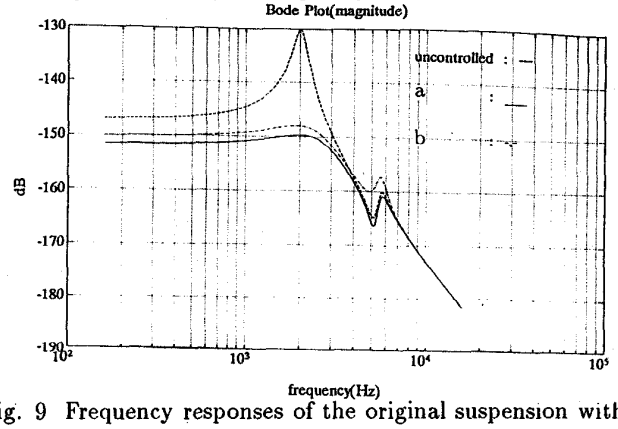

Fig. 9 Frequency responses of the original suspension without optimization (control input at a: solid curve, b: dashdot curve, and uncontrolled system: dashed curve)

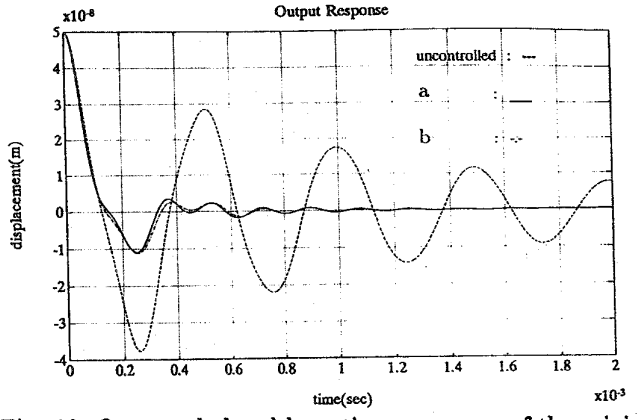

Fig. 10 Open and closed-loop time responses of the original suspension without optimization (control input at a: solid curve, b: dashdot curve, and uncontrolled system: dashed curve)

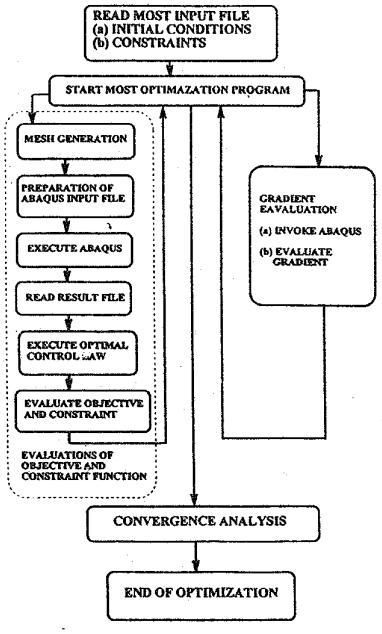

Fig. 11 Computation flow of structure/control optimization

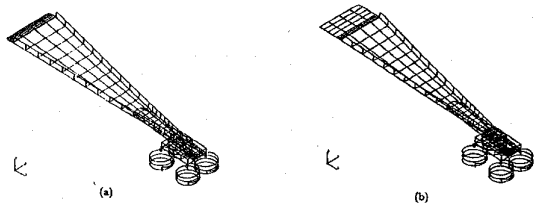

Fig. 12 Optimal structure/control design results (a) goal programming ($\beta = 1$) (b) compromise programming ($\gamma = 1$)

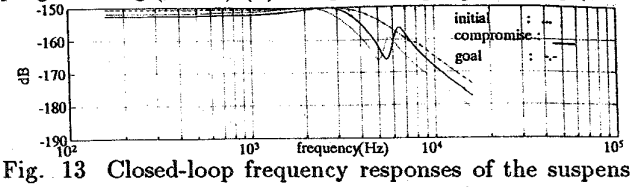

Fig. 13 Closed-loop frequency responses of the suspension with integrated structure/control design (solid curve: compromise programming, dashdot curve: goal programming, dotted curve: original suspension with optimal control)

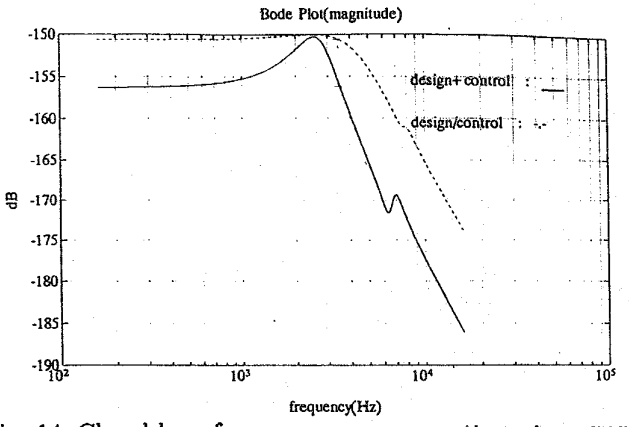

Fig. 14 Closed-loop frequency responses with goal programming designs ($\beta = 1$)

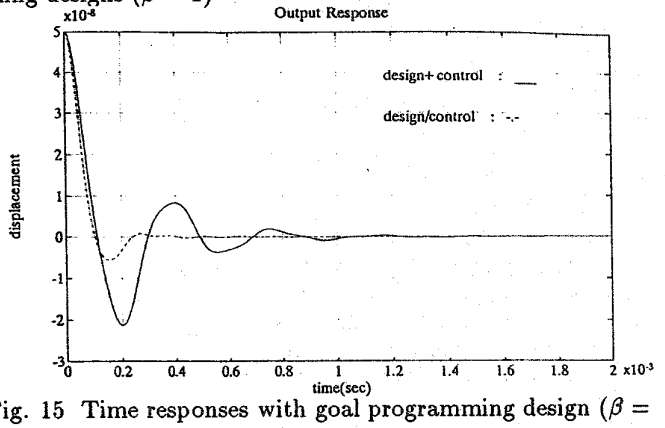

Fig. 15 Time responses with goal programming design ($\beta = 1$)

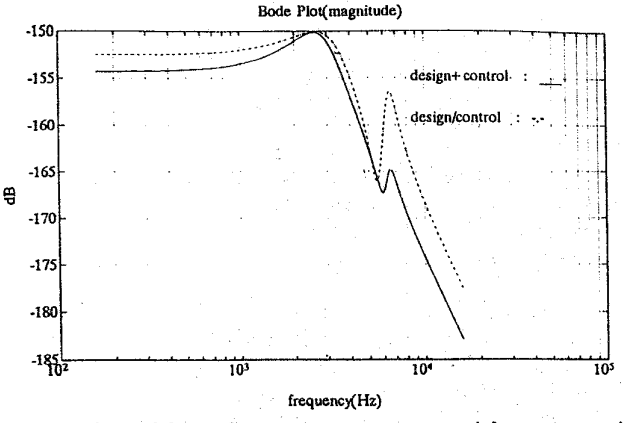

Fig. 16 Closed-loop frequency responses with compromise programming designs ($\gamma = 1$)

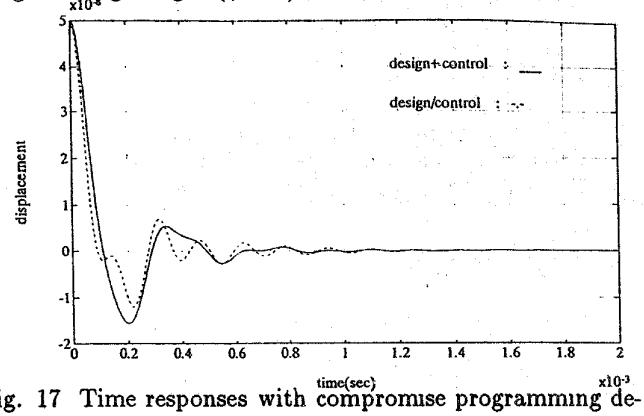

Fig. 17 Time responses with compromise programming design ($\gamma = 1$)